electronics

Article

Experimental Study of Electric Power Generation with Concentrated Solar Thermoelectric Generator

Mohammed Bensafi [1], Houari Ameur [2,*], Noureddine Kaid [1,2], Siamak Hoseinzadeh [3,*], Saim Memon [4,5] and Ali Sohani [6]

[1] Laboratory of Energetic in Arid Zones (ENERGARID), University Tahri Mohamed of Bechar, P.O. Box 417, Bechar 08000, Algeria; bensafi.med08@gmail.com (M.B.); kaid.noureddine2@gmail.com (N.K.)
[2] Department of Technology, University Centre of Naama-Salhi Ahmed, P.O. Box 66, Naama 45000, Algeria
[3] Department of Planning, Design, Technology of Architecture, Sapienza University of Rome, 00196 Rome, Italy
[4] Solar Thermal Vacuum Engineering Research Group, London Centre for Energy Engineering, School of Engineering, London South Bank University, 103 Borough Road, London SE1 0AA, UK; s.memon@lsbu.ac.uk
[5] Department of Engineering and Technology, School of Computing and Engineering, University of Huddersfield, Huddersfield HD1 3DR, UK
[6] Laboratory of Optimization of Thermal Systems' Installations, Faculty of Mechanical Engineering-Energy Division, K.N. Toosi University of Technology, No. 15–19 Pardis St., Mollasadra Ave., Vanak Sq., Tehran 1999-143344, Iran; alisohany@yahoo.com
* Correspondence: ameur.houari@cuniv-naama.dz (H.A.); siamak.hosseinzadeh@uniroma1.it (S.H.)

Abstract: Although thermoelectric technology is little-known in the public domain, it presents an exciting alternative solution in many cases where lost heat energy can be quickly recovered to produce electricity. In the present paper, an attempt is undertaken to exploit this energy. For this purpose, an experimental study is conducted to produce electricity with the thermoelectric effect by utilizing a device placed on a parabolic concentrator. The device is placed on a solar tracker. The results obtained for two days of two distinct months, January and June, revealed that the production in June was higher than that in January by around 92.86%. This distinction is due to the concentrated solar beam being different on a day in each month. A vital product was recorded by utilizing the concentrator. This gadget permitted us to take advantage of the limit of sun-based radiation to produce power. The power may be stored with a legitimate stockpiling procedure.

Keywords: thermoelectric effect; solar power; concentrator; solar tracker; electricity production

check for updates

Citation: Bensafi, M.; Ameur, H.; Kaid, N.; Hoseinzadeh, S.; Memon, S.; Sohani, A. Experimental Study of Electric Power Generation with Concentrated Solar Thermoelectric Generator. *Electronics* **2022**, *11*, 1867. https://doi.org/10.3390/electronics11121867

Academic Editor: Rui Castro

Received: 27 April 2022
Accepted: 8 June 2022
Published: 13 June 2022

Publisher's Note: MDPI stays neutral with regard to jurisdictional claims in published maps and institutional affiliations.

Copyright: © 2022 by the authors. Licensee MDPI, Basel, Switzerland. This article is an open access article distributed under the terms and conditions of the Creative Commons Attribution (CC BY) license (https://creativecommons.org/licenses/by/4.0/).

1. Introduction

Thermoelectric effects were discovered during the 19th century. The two most "famous" are the Seebeck effect and the Peltier effect. Still, many other thermoelectric effects are associated with the simultaneous application of a field, a magnetic or electric current, such as the Nernst effect, the Thomson effect, or the Ettingshausen effect [1]. The conversion $\Delta T \rightarrow \Delta V$ via the Seebeck effect or $\Delta V \rightarrow \Delta T$ via the Peltier effect also make it possible to provide applications of these materials in the fields of electricity production or refrigeration. The efficiency of a thermoelectric module for these applications is defined as the "merit factor", ZT. It is compared to the Carnot yield (excellent yield of a thermodynamic device operating between a hot temperature, T_c, and a cold temperature, T_f, and defined as $((T_c - T_f)/T_c)$). For Seebeck modules, the maximum efficiency can reach 10% of the Carnot efficiency for ΔT = 700 K, with T_f = 300 K and ZT = 1 (18% if ZT = 2).

At present, thermoelectric modules are used in niche areas, such as spaces or locations far from conventional electrical distribution circuits (in the mountains, for communication systems on pipelines, etc.). These generators are widely used in space applications, particularly those based on PbTe or SiGe used on board since 1961 by NASA, or more recently for the Curiosity mission to Mars. In this area, thermoelectric technology has

shown effectiveness, since thermogenerators have been operating for 30 years with low power losses, for example, in Voyager probes. In addition, an advantage of this technique is that the modules are not subjected to any mechanical movement and do not use fluid, making this technology very reliable and robust. Another large-scale application is the air conditioning of car seats in the United States and Canada using Peltier coolers. Only the active seats are targeted, which avoids unnecessary air conditioning throughout the vehicle. Thermoelectricity has experienced renewed interest over the past fifteen years, and many projects are under study. Thus, it is possible to equip stoves, water heaters, or lamps with thermogenerators, then to supply small electrical equipment independently.

Gould et al. [2] developed a review paper covering a basic theory of the construction and operation of the thermoelectric modules. It includes their advantages and disadvantages, and a market analysis with a brief overview and presentation of the results of a thermoelectric test system. They concluded that thermoelectricity could be used for cooling and heating in electricity production. Climate change issues are predicted to contribute to the development of thermoelectricity in the coming years, as reported by these authors.

A correlation between the thermoelectric measurements of the power coefficient and the induced impedance was given by the nondestructive evaluation of the residual stress on machined uranium surfaces [3]. Thus, Vanhorn et al. [3] measured the thermoelectric power by using a nondestructive contact probe to evaluate the near-surface defects. They concluded that the thermoelectric power coefficient could measure the residual stress to locate the surface regions damaged by machining. The thermoelectric power coefficient probes could measure the deformation for noncontact use. Lara et al. [4] used the thermoelectric power (TEP) values as an essential process to predict the metallurgical state of different alloys. They measured the evolution of the thermoelectric power coefficient on isothermally aged 2205 duplex stainless steel. Kraemer et al. [5] developed a solar thermoelectric generator (STEG) that achieved a peak efficiency of 4.6% under AM1.5G (1 $kW \cdot m^{-2}$) conditions. The effectiveness obtained was about seven to eight times higher than the previously reported best cost value for a flat-panel STEG. Yang et al. [6] presented an experimental realization of using abundant and nontoxic copper, zinc, and tin sulfide (CZTS) nanocrystals for potential thermoelectric applications.

Granule blasting is a surface procedure technique generally applied to increase the technical fixation on implants by maximizing their very own sharpness. Based on this technique, Carreon et al. [7] blew up two metallic biomaterial alloys, 316LVM and Ti6Al4V, by projecting particles of Al_2O_3 and ZrO_2, which gave a rough and fine surface, respectively. It was found that these TEP dimensions were connected directly using the variations of the subtle material.

To examine conveniently and through self-confidence the level of sensitization (DOS) throughout duplex stainless steel (DSS), a nondestructive approach was discovered. In this circumstance, Ortiz et al. [8] stated that the TEP coefficient was sensitive to continuous microstructural adjustments generated with thermal aging, and could be utilized to display the IGC sensitization of 2205 duplex stainless steel.

Bismuth telluride is the most standard component utilized for thermoelectric refrigeration. It illustrates the most apparent thermoelectric creation at a medium operating heat source temperature. Goldsmid [9] discussed the likely temperature dependence of the thermoelectric parameters and how the composition may be optimized for applications above room temperature.

The actual efficiency of the solar panel decreases as its temperature increases. Consequently, the actual result strength of the PV module falls with the augmentation in the temperature if the heat is not eliminated. Some well-developed techniques for this issue were presented by Dinesh et al. [10], where they demonstrated the benefit of thermoelectric cooling to enhance the PV module's performance. They reported that the efficiency and life improvement of the PV component might be reached with 25 °C cooling devoid of a loss of power. Kraemer et al. [11] provided an experimental evaluation of solar thermoelectric

generators (STEGs) with the highest productivity of 9.6% from an optically concentrated standard solar irradiance of 211 $kW \cdot m^{-2}$ and a system efficiency of 7.4%.

Approximately 30% of fuel energy is rejected through the exhaust, so it is expected to utilize wasted energy to the extent of its potential. Rathore et al. [12] reported that the recovery and use of waste heat not only retains fuel, but also decreases the quantity of waste heat and greenhouse gases trashed into the natural environment. The evidence from this study points towards the idea that waste heat treatment techniques implement a thermoelectric power generator that may be applied for fueling numerous low electric energy intake parts of a vehicle process, making use of the exhaust gas supply energy correctly.

To manufacture a high-efficiency thermoelectric device for low electrical contact resistance, Sallehin et al. [13] studied the electrical contact between thermoelectric segments as an interface layer or assembly technique for a segmented leg. Pustan et al. [14] presented an analysis of the temperature effect on the mechanical properties of titanium dioxide thin films. The circulating laser deposited the films at three different oxygen pressures, with changed film thicknesses depending on the installation pressure. They used this material in a thermoelectric application under different temperature gradients, and they conducted tests at temperatures between 20 °C and 100 °C. The obtained results showed a decrease in both mechanical properties with increasing temperature. Mukherjee et al. [15] inspected the thermoelectric properties of CuS nanoparticles synthesized with a simple polyol-based method using CTAB and PVP as surfactants. They noted that the presence of surfactants during the synthesis of CuS nanoparticles seemed to prevent the volatility of sulfur, which caused the capped samples to become S-rich and, thus, improved the electrical conductivity and thermal power. A significant improvement of more than 50% in the thermoelectric power factor at 300 K was observed for CuS nanoparticles capped with CTAB and PVP compared to the pure ones.

The thermoelectric pump is the primary unit of a thermoelectric cooling system. For the Peltier module to work efficiently, the thermal power produced on its hot side must be dissipated by a heat sink and a fan. Belovski et al. [16] considered a method for calculating the thermal resistance of aluminum and copper heat sinks with parallel plates. The two materials were compared for the number and length of fins. Jaziri et al. [17] reported optimizing the design of thermoelectric generators based on low-temperature cosintered ceramic technology. Nassar et al. [18] reported an experimental investigation of a forced convective pulsating flow of the air and magnetic field effect on the thermoelectric cooler performance with a Reynolds number of 5871. Their results showed that the temperature differences were between 5.56 °C and 19.8 °C. In addition, the thermoelectric cooler's coefficient of performance ranged from 0.122 to 0.277. Min et al. [19] predicted the existence of significant effects beyond room temperature in a thermoelectric fast-ion conductor Cu_2Se through classical molecular dynamics simulations and first-principle computational methods. Their simulation results showed that the thermoelectric compounds presenting a high ionic disorder, such as copper and silver-based chalcogenides, may render significant mechanocaloric effects and, thus, are promising materials for engineering solid-state cooling applications that do not require the use of electric fields. Other interesting works may be found in Refs. [20–26].

Some works presented the structural and electronic band properties of GeTe and compared it with GeTe with low-temperature, high-symmetry, and high-temperature cubic surfaces. GeTe had a low-energy displacement between L and valence band points, reaching a high thermal performance through a direct bandgap and phonon array velocity. Liu et al. [27] conducted an applicable work that fundamentally explored to set up a connection between progress metal doping, an electronic quality element, and the figure-of-value of GeTe. From the first-standard estimations, it was discovered that Ta, as an unseen dopant in GeTe, can successfully join the energy offset among light and bulky conduction band extrema to upgrade powerful mass at high temperatures.

In light of the quick improvement of fiber-based thermoelectrics, an audit [28,29] meant to exhaustively sum up the cutting-edge fiber-based thermoelectric materials and

gadgets, including their one-of-a-kind plans and synthetic designing, progressed creation techniques, exceptional thermoelectric properties, and wide applications. Nazari et al. [30] elucidated the performance of a copper oxide (Cu_2O) nanofluid in a single-slope solar still integrated with an external thermoelectric glass cover cooling channel. The results revealed that the modified solar productivity, energy efficiency, and exergy efficiency were still enhanced compared with the traditional solar still. With the addition of a 0.08% volume fraction of Cu_2O nanoparticles to the basin water of a modified solar still with the thermoelectric cooling channel, the highest enhancement values for productivity, energy, and exergy efficiencies were approximately 81%, 80.6%, and 112.5%, respectively.

Thermoelectric effects make it possible to transform a temperature difference, ΔT, into a difference in potential electric, ΔV, via the Seebeck effect, or ΔV into ΔT via the Peltier effect. These two effects are suitable probes of the electronic structure of materials. They can be used to transform waste heat into electricity (Seebeck mode in the case studied) or to manufacture coolers (Peltier mode). These various thermoelectric effects are well-informed in condensed matter physics, because their transport properties are extremely sensitive to a material's electronic structure. They constitute suitable probes for studying carriers, their density of states, and their different diffusion mechanisms (charge diffusion on the atomic network via phonons, scattering by spins, and distribution between charges). In our study, we take advantage of the region's solar potential (the area of Bechar, Algeria). At the focal point of the concentrator, we placed the thermopile. The concentrator tracked the solar beam all day. The obtained results show the work's originality, which could be helpful in many positions and several research areas.

The amount of solar radiation in our region is vast; therefore, our contribution is to make worthwhile use of it by extracting high heat through a concentrator and putting it directly into a thermoelectric device to produce electricity. The experience that we created used a limited number of wires. Therefore, the results are not encouraging compared to the desired results. However, in fact, we speak of a vast and unused solar area that could use many concentrators that can produce large quantities of electric power.

2. Thermoelectric Theory

2.1. Seebeck Effect

Two materials a and b of different natures were connected by two temperature junctions T. One of the junctions was heated to temperature T_1, such that $T_1 > T$. A voltage difference then appeared between the cold and hot junctions.

Let us now consider a and b as n-type and p-type semiconductors, respectively. The Seebeck effect is explained by the charge carrier diffusion, e− (electrons) or e+ (hole) from the hot side to the cold side. For an open circuit, the e− (electrons) are massed in the cold part of the n-type material, while the e+ (hole) are huddled in the cold part of the p-type material. Therefore, the cold part of the semiconductor n would be negatively polarized, and the cold part of the semiconductor p positively polarized. Consequently, we would have a difference in charges, which has the effect of generating a difference in the potential between the two cold ends of these materials.

2.2. Peltier Effect

If a current is passed through a circuit with two different conductors joined at the same temperature, heat would absorb in one junction and then be released.

Let us now consider a and b as n-type and p-type semiconductors, respectively. The junction that absorbs heat would then be the one in which the current passes from the n-type material (b) to the p-type material (a), i.e., the junction at temperature T_1.

Conversely, the one that returns it is the junction in which the current passes from the p-type material (a) to the n-type material (b).

2.3. Thomson Effect

The third thermoelectric effect (the Thomson effect) is highlighted when a temperature gradient and electric current are present simultaneously.

A material subjected to a temperature gradient and an electric current would exchange heat with the outside environment, either resulting in an absorption of heat from the outdoor environment when the current flows in the opposite direction of the temperature difference or a release of heat when the current flows in the direction of the temperature difference.

2.4. Seebeck Coefficient

A temperature difference dT at the junctions of two materials a and b implies an electrical potential difference dV according to:

$$S_{ab} = \frac{dv}{dT} \tag{1}$$

The Seebeck coefficient, also known as the "thermoelectric power", is expressed in $V \cdot K^{-1}$ (or, more generally, in μV/K in view of the values of this coefficient in common materials).

The Seebeck coefficients of both materials are related to the Seebeck coefficient of the torque according to:

$$S_{ab} = S_a - S_b \tag{2}$$

2.5. Peltier Coefficient

In the case of the Peltier effect, an electric current I is imposed on a circuit composed of two materials, resulting in a heat release Q at one junction and a heat absorption at the other junction, according to:

$$\pi_{ab} = \frac{Q}{I} \tag{3}$$

2.6. Thomson Coefficient

The Thomson coefficient can be defined directly for a single material. When a temperature gradient and an electric current are present simultaneously, heat is generated or absorbed in every single material segment. The heat flow gradient within the material is then given by:

$$\frac{dQ}{dx} = I\tau\frac{dT}{dx} \tag{4}$$

where x is the spatial coordinate and τ is the Thomson coefficient of the material.

The calculation method of the power is given by:

$$P = V_c\left(I_{ph} - I_a \cdot \exp\left(\frac{q}{A \cdot K \cdot T}V_c - 1\right)\right) \quad (W) \tag{5}$$

$$I_c = I_{ph} - I_0 \cdot \exp\left(\frac{q}{A \cdot K \cdot T}V_c - 1\right) \quad (A) \tag{6}$$

3. Solar Radiation in the Region of Bechar

Geographically, solar energy received is unevenly distributed. In the world's hottest regions, annual sunshine can reach 2300 $kWh/m^2 \cdot year$ (energy received by a surface area of 1 m^2 during one year). In our region, the average sunshine is 2100 $kWh/m^2 \cdot year$. By comparison, 1 L of fuel oil contains 10 kWh.

Figures 1–3 present the temperature values, the global solar radiation on a horizontal plane, and the concentrated radiation obtained by the ENERGARID laboratory metrology station, respectively. These parameters are presented for January and June (21 June). The instrument we used to measure the radiation was the Kipp & Zonen (Delft, The Netherlands) 2AP.

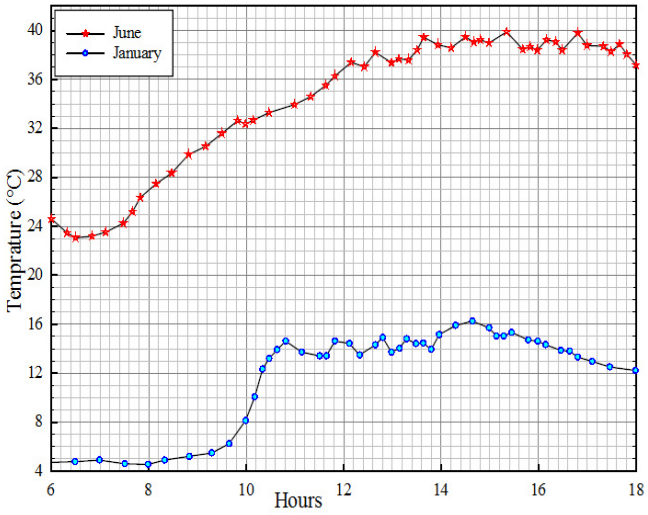


Figure 1. Variations of the temperature vs. time in January and June.

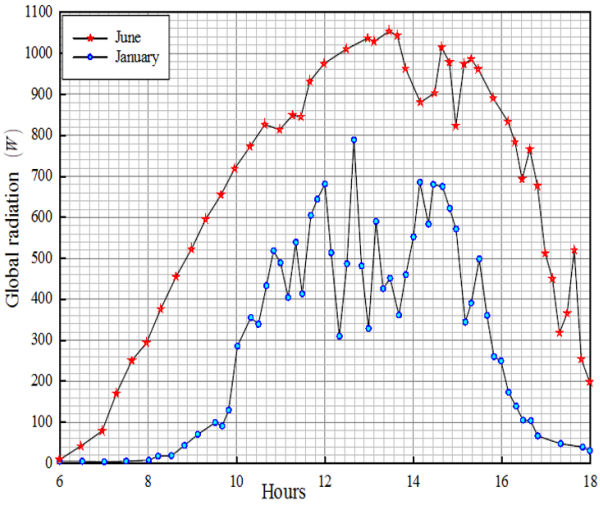


Figure 2. Variations of the global radiation vs. time in January and June.

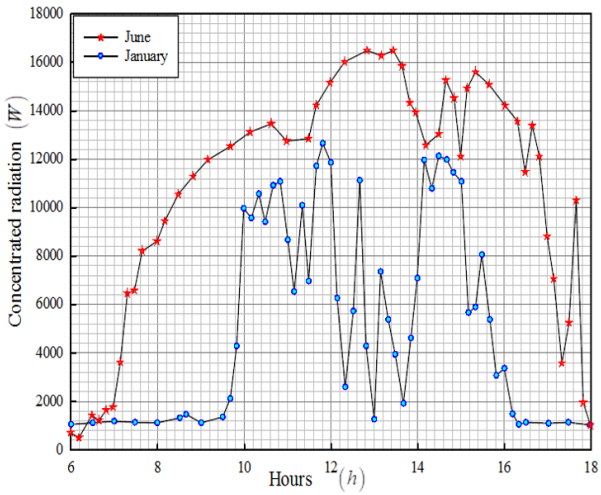


Figure 3. Variations of the concentrated radiation vs. time in January and June.

In Figure 3, we measured the concentration radiation flux using the instrument of measurement, Kipp & Zonen 2AP. The obtained solar radiation flux was approximately 18,000 w/m^2.

4. Experimental Setup

Copper oxide is a kind of compound that forms on pieces of copper when you heat them with a flame (Figure 4). In addition to being used for other things, such as the manufacture of photosensors, thermistors, pressure sensors, and diodes, it can also be used to create an impressive thermoelectric junction capable of producing hundreds of millivolts when heated with a flame.

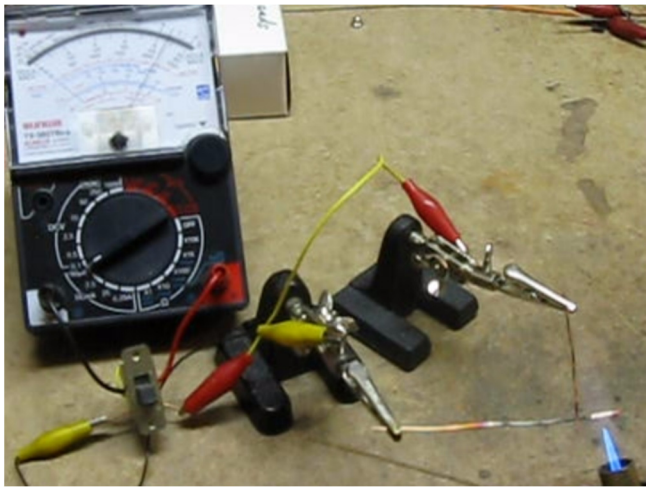


Figure 4. Thermoelectric copper oxide generator.

The solar tracker is a device that tracks the position of the sun. The solar concentrator collects the solar flux into a focal place. Therefore, in this experience, we put the thermoelectric device in a focal position of the concentrator, which was put on the solar tracker.

The metal parts were composed of 10 bare copper wires and were 4 cm long from the hot ends to the hairpin ends. The L-shaped curves were 3 cm from the burning tip (Figure 5). The support was an assembly of metal, a layer of insulation for all the pieces of wire, and a circular hole in the central section of the cutout 6 cm in diameter. All parts of the copper wire were mounted at 36-degree intervals within the space around the circle. Each L-shaped wire was the positive cold side of a joint, and each straighter piece was the hot negative side of a joint. The thermoelectric junctions were formed with copper oxide between each piece of straight wire and the L-shaped piece, which rested on top of it.

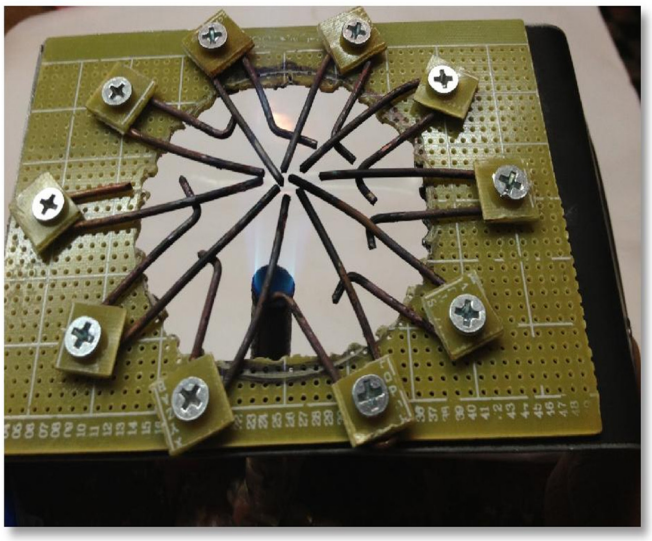
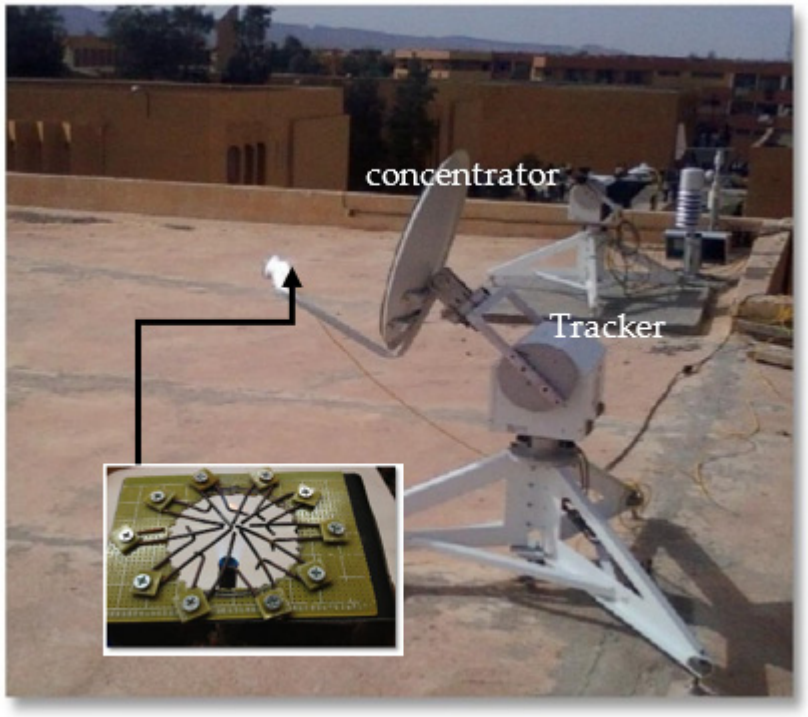
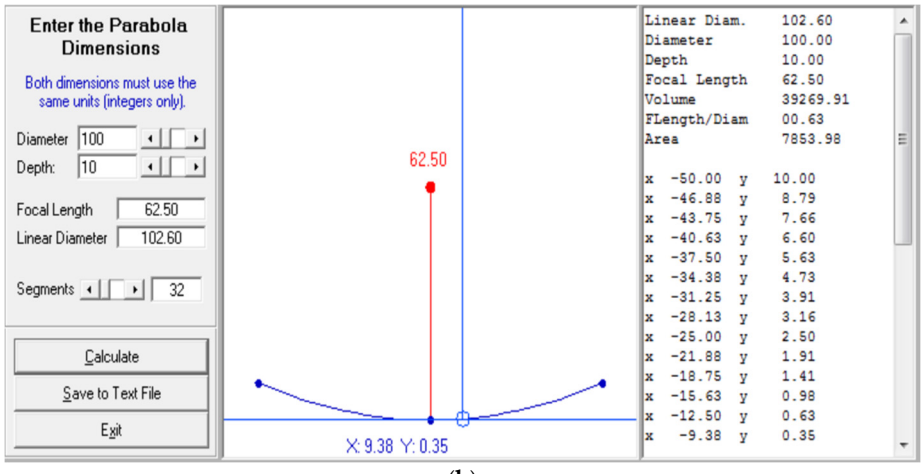


Figure 5. Thermocouple.

The thermoelectric device was placed on a solar concentrator, and the whole system was set on a solar tracker to ensure a maximum solar concentrator beam (Figure 6). Recently, TEGs have received increasing attention as a green and flexible power source that can meet a wide range of power needs, from thermocouple sensors to satellite generators. Thermoelectric generators have a low-conversion efficiency; however, if used to harness waste heat from industrial processes or central heating systems, or high temperatures of concentrators, they could be a promising solution.



(**a**)



(**b**)

Figure 6. (**a**): Concentrator. (**b**): Concentrator characteristics.

The concentration factor for the parabolic concentrated collector is detailed in Figure 6b and Equation (7).

The equation of concentrator geometric is given by:

$$y = 4 \cdot f \cdot x^2 \tag{7}$$

with f (the focal distance) given by:

$$p = \frac{2f}{1 + \cos\psi} \tag{8}$$

p: concentrator radius.

ψ: angle measured from the line (from center to focal point) and the concentrator radius (P).

5. Electric Production

Current and potential applications of thermoelectric materials take advantage of both aspects of the Thomson effect. On the one hand, the establishment of a heat flow, as opposed to thermal diffusion, when current flow through semiconductor material (thermoelectric), that makes it possible to suggest refrigeration applications. This alternative solution to conventional refrigeration using compression–expansion cycles does not require moving parts, resulting in better reliability and less vibration and noise. These properties are fundamental in applications where the temperature must be regulated very precisely and reliably, for example, in containers used to transport organs to be transplanted, or for applications where vibrations are a considerable nuisance, such as laser guidance systems or integrated circuits. In addition, the possibility of creating a heat flow from an electric current as soon as it makes use of freon-type gases, which contribute to the degradation of the ozone layer, is unnecessary. Since 2000, there has been an important market for refrigeration with thermoelectricity for portable coolers connected to 12-volt electric current vehicles.

On the other hand, the possibility of converting a flow of heat into an electric current makes it possible to envisage applications for generating electricity with the thermoelectric effect, in particular from waste heat sources such as automobile exhaust pipes (saving 5% to 10% of the expected fuel by limiting the use of the alternator), incinerator stacks, cooling circuits in nuclear power stations, etc. Thermoelectric systems would then constitute "clean" backup energy sources using new heat sources. Moreover, the systems' very high reliability and durability (thanks to the absence of moving parts) have led to their use for the power supply of space probes. This is notably the case of the Voyager probe, launched in 1977, in which the heat flow established between fissile PuO_2 (PuO_2 is radioactive and decays, so it is a source of heat) and the external environment passed through a thermoelectric conversion system based on SiGe (an alloy of silicon and germanium), allowing the probe to be supplied with electricity (in fact, space probes that are too far from the sun cannot be powered by solar panels, as the solar flux becomes too weak).

The efficiency of electricity production was low due to the material used in this experiment, except that we used a parabolic concentrator that followed the sun during the day (the focal point was focusing on the thermoelectric device during the day), increasing the production of electricity with efficiency.

Values of the hourly electric production for January and June are presented in Figure 7 (one element). The efficiency of electricity production was low due to the material used in this experiment, except that we used a parabolic concentrator and that the concentrator followed the sun during the day. (The instrument was the Kipp & Zonen professional instrument).

The values of the hourly electric production of 16 elements for January and June are presented in Figure 8. The efficiency of electricity production was essential due to the material and the number of components used in this experiment. Moreover, we used a parabolic concentrator, which followed the sun during the day (Figures 9 and 10). At midday, the maximum voltage value is shown in Figures 8 and 9. This value was the result of the top solar radiation. In the experiment, the cold-side temperature of the thermocouple was the ambient temperature shown in Figure 1, and the hot temperature was the temperature given by the concentrator.

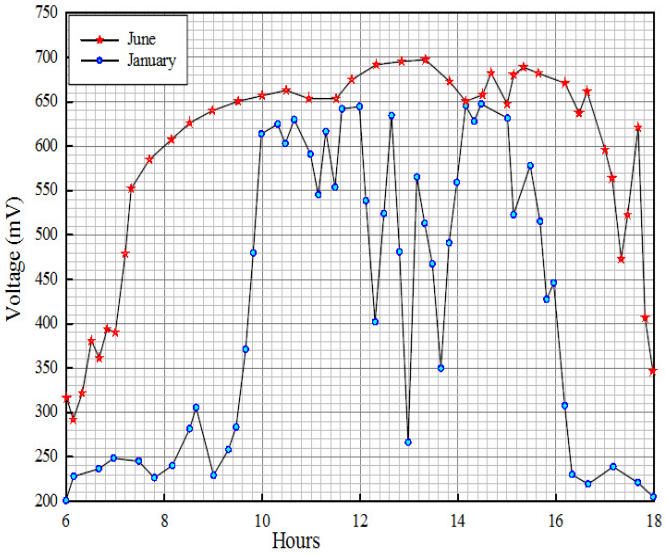


Figure 7. The hourly electric production in January and June (for one element).

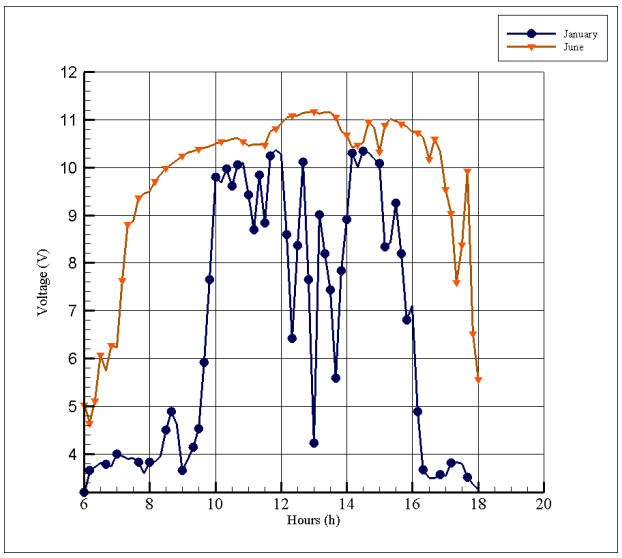


Figure 8. The hourly electric production in January and June (for 16 elements).

The results shown in Figure 8 are for the thermoelectric element placed in the concentrator.

We note that we measured the potential difference in the experiment that the electric production was given in voltage.

Figure 10 presents the power production for one element (the wire size was 10 mm in length by 1 mm of section). Therefore, the production would increase when using more than one element.

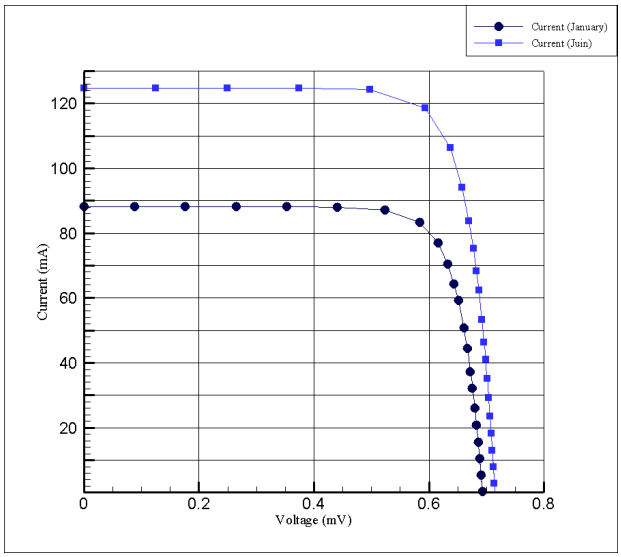


Figure 9. Open-circuit voltage and current testing graphs in January and June.

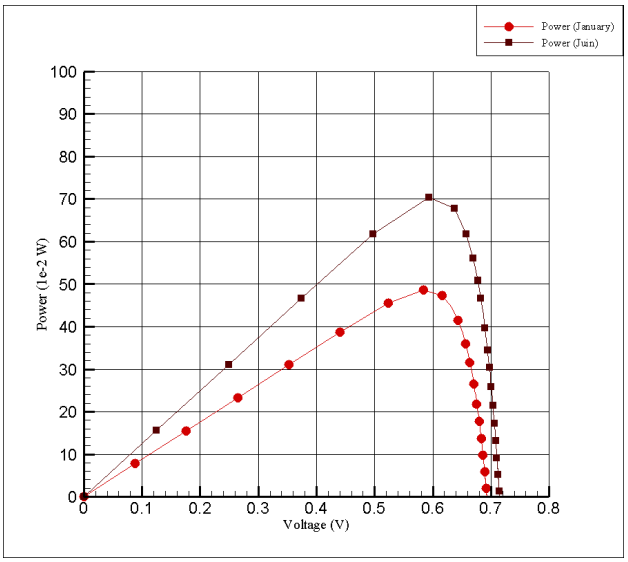


Figure 10. Open-circuit voltage and power testing graphs in January and June.

6. Conclusions

Conversion systems using the thermoelectric effect had low efficiencies, limiting thermopiles to a few applications where reliability and durability are more important than the cost and performance, such as that used in greenhouses, in the tents of desert dwellers (Nomads), and as a source of energy production for weather stations planted in arid places. Thermoelectric generators allow for recharging portable devices (batteries of mobiles) in the case of a mains failure, as was the case in New York during Hurricane Sandy. In general, it can be used as a source of electrical energy, where the solar panels cannot give enough output from the electrical output. As it is known, solar panels in harsh conditions and high temperatures do not provide the desired results as an energy source. Accordingly, with more studies and experiments, thermoelectric cells are considered an alternative to energy sources, or they can at least be combined with solar panels. Thus, an effective system can be configured that gives satisfactory results.

The Bechar (Algeria) region benefits from a sunny climate during the year. The average day length in the summer season is more than 12 h of sunshine (the duration of the recording of electricity production). The obtained results for two days of two different months, January and June, revealed that the production in June was higher than

that in January by approximately 92.86%. This difference in production was due to the concentrated flow for the two months. A significant production was recorded by using the concentrator. This device allowed us to exploit the maximum solar radiation to generate electricity, and the electricity may be stored with a proper storage technique.

Author Contributions: Conceptualization, M.B.; methodology, M.B., N.K. and S.H.; software, M.B.; validation, M.B. and H.A.; formal analysis, H.A., S.H., S.M. and A.S.; funding, H.A., S.H., S.M. and A.S.; investigation, M.B., H.A., S.H., S.M. and A.S. data curation, H.A., N.K. and S.H.; writing-original draft preparation, M.B., H.A. and N.K.; writing-review and editing, H.A., S.H., S.M. and A.S.; resources, M.B. and N.K. All authors have read and agreed to the published version of the manuscript.

Funding: This research received no external funding.

Institutional Review Board Statement: Institutional Review Board Statement and approval number are not applicable.

Informed Consent Statement: No informed consent statement was required for this study.

Data Availability Statement: All data are available in the manuscript.

Conflicts of Interest: The authors declare no conflict of interest.

References

1. Sifi, I.; Kaid, N.; Ameur, H.; Inc, M.; Baleanu, D.; Menni, Y.; Lorenzini, G. Comparison between the thermoelectric properties of new materials: The alloy of iron, vanadium, tungsten, and aluminum (Fe2V0.8W0.2Al) against an oxide such as $NaCO_2O_4$. *Optik* **2021**, *247*, 168035. [CrossRef]
2. Gould, C.A.; Shammas, N.Y.A.; Grainger, S.; Taylor, I. A comprehensive review of thermoelectric technology, micro-electrical and power generation properties. In Proceedings of the 2008 26th International Conference on Microelectronics MIEL, Nis, Serbia, 11–14 May 2008; pp. 329–332. [CrossRef]
3. Vanhorn, C.A.; Olson, D.L.; Mishra, B.; Jackson, J.E.; Evans, K. Assessing residual stress on machined uranium using non-destructive thermoelectric power coefficient and induced impedance measurements. *AIP Conf. Proc.* **2009**, *1096*, 1317–1324. [CrossRef]
4. Lara, N.; Ruiz, A.; Carreón, H.; Medina, A.; Sánchez, A. Study of aging effects in 2205 duplex stainless steel using thermoelectric power measurement. *AIP Conf. Proc.* **2010**, *1211*, 1333–1339. [CrossRef]
5. Kraemer, D.; Poudel, B.; Feng, H.P.; Caylor, J.C.; Yu, B.; Yan, X.; Ma, Y.; Wang, X.; Wang, D.; Muto, A.; et al. High-performance flat-panel solar thermoelectric generators with high thermal concentration. *Nat. Mater.* **2011**, *10*, 532–538. [CrossRef]
6. Yang, H.; Jauregui, L.A.; Zhang, G.; Chen, Y.P.; Wu, Y. Nontoxic and abundant copper zinc tin sulfide nanocrystals for potential high-temperature thermoelectric energy harvesting. *Nano Lett.* **2012**, *12*, 540–545. [CrossRef]
7. Carreon, H.; Ruiz, A.; Barriuso, S.; González-Carrasco, J.L.; Caballero, F.G.; Lieblich, M. Nondestructive thermoelectric evaluation of the grit blasting induced effects in metallic biomaterials. *AIP Conf. Proc.* **2013**, *1511*, 1504–1511. [CrossRef]
8. Ortiz, N.; Carreón, H.; Ruiz, A. NDE evaluation of the intergranular corrosion susceptibility of a 2205 duplex stainless steel using thermoelectric power and double loop electrochemical potentiokinetic reactivation methods. *AIP Conf. Proc.* **2013**, *1511*, 1264–1269. [CrossRef]
9. Goldsmid, H.J. Bismuth telluride and its alloys as materials for thermoelectric generation. *Materials* **2014**, *7*, 2577–2592. [CrossRef]
10. Borkar, M.D.S.; Prayagi, D.S.V.; Gotmare, M.J. Performance Evaluation of Photovoltaic Solar Panel Using Thermoelectric Cooling. *Int. J. Eng. Res.* **2014**, *3*, 536–539. [CrossRef]
11. Kraemer, D.; Jie, Q.; Mcenaney, K.; Cao, F.; Liu, W.; Weinstein, L.A.; Loomis, J.; Ren, Z.; Chen, G. Concentrating solar thermoelectric generators with a peak efficiency of 7.4%. *Nat. Energy* **2016**, *1*, 1–8. [CrossRef]
12. Rathore, S.S.; Singh, A.; Kumar, P.; Alam, N.; Sahu, M.K.; Sanjay, R. Review of Exhaust Gas Heat Recovery Mechanism for Internal Combustion Engine Using Thermoelectric Principle. *SAE Tech. Pap.* **2018**, *2018*, 1–10. [CrossRef]
13. Sallehin, N.Z.I.M.; Yatim, N.M.; Suhaimi, S. A review on fabrication methods for segmented thermoelectric structure. *AIP Conf. Proc.* **2018**, *1972*, 030003. [CrossRef]
14. Pustan, M.; Birleanu, C.; Merie, V.; Garabagiu, S.; Marconi, D.; Barbu-Tudoran, L.; Voicu, R. Thermal Effect on Mechanical Properties of Titanium Oxide Thin Films for Thermoelectric Applications. In Proceedings of the 2019 Symposium on Design, Test, Integration & Packaging of MEMS and MOEMS (DTIP 2019), Paris, France, 12–15 May 2019; pp. 1–4. [CrossRef]
15. Mukherjee, B.; Tarachand; Hussain, S.; Okram, G.S. Effect of different surfactants on thermoelectric properties of CuS nanoparticles. *AIP Conf. Proc.* **2019**, *2100*, 020091. [CrossRef]
16. Belovski, I.; Aleksandrov, A. Determination of the thermal resistance of aluminum and copper heat sink in a thermoelectric pump. In Proceedings of the 2019 16th Conference on Electrical Machines, Drives and Power Systems (ELMA 2019), Varna, Bulgaria, 6–8 June 2019; pp. 1–4. [CrossRef]

17. Jaziri, N.; Boughamoura, A.; Muller, J.; Tounsi, F.; Mezghani, B.; Kouki, A. TCs connectivities effect investigation in the LTCC-based thermoelectric generator for automotive waste heat recovery. In Proceedings of the IEEE International Conference on Design & Test of Integrated Micro & Nano-Systems, Tunis, Tunisia, 28 April–1 May 2019; pp. 1–5. [CrossRef]
18. Nassar, M.S.; Hegazi, A.A.; Mousa, M.G. Combined effect of pulsating flow and magnetic field on thermoelectric cooler performance. *Case Stud. Therm. Eng.* **2019**, *13*, 3–12. [CrossRef]
19. Min, J.; Sagotra, A.K.; Cazorla, C. Large barocaloric effects in thermoelectric superionic materials. *Phys. Rev. Mater.* **2020**, *4*, 1–10. [CrossRef]
20. Sifi, I.; Ghellai, N.; Menni, Y.; Chamkha, A.; Ameur, H. Analysis and modeling of thermoelectric modules based on skutterudites family. *Tec. Ital.-Ital. J. Eng. Sci.* **2020**, *64*, 91–94. [CrossRef]
21. Rachedi, M.; Merad, A.; Lorenzini, G.; Ahmad, H.; Menni, Y.; Ameur, H.; Sifi, I. Effect of the properties of chalcopyrite semiconductors on the physical and optical parameters of cell layers with CIGS. *Rev. Compos. Matériaux Av.-J. Compos. Adv. Mater.* **2021**, *31*, 65–72.
22. Deng, L.; Li, Y.; Cai, W.; Haselhuhn, A.S.; Carlson, B.E. Simulating thermoelectric effect and its impact on asymmetric weld nugget growth in aluminum resistance spot welding. *J. Manuf. Sci. Eng.* **2020**, *142*, 091001. [CrossRef]
23. Zoui, M.A.; Bentouba, S.; Stocholm, J.G.; Bourouis, M. A review on thermoelectric generators: Progress and applications. *Energies* **2020**, *13*, 3606. [CrossRef]
24. Jouhara, H.; Żabnieńska-Góra, A.; Khordehgah, N.; Doraghi, Q.; Ahmad, L.; Norman, L.; Axcell, B.; Wrobel, L.; Dai, S. Thermoelectric generator (TEG) technologies and applications. *Int. J. Thermofluids* **2021**, *9*, 100063. [CrossRef]
25. Wang, J.; Xiao, F.; Zhao, H. Thermoelectric, piezoelectric and photovoltaic harvesting technologies for pavement engineering. *Renew. Sustain. Energy Rev.* **2021**, *151*, 111522. [CrossRef]
26. Ge, M.; Li, Z.; Wang, Y.; Zhao, Y.; Zhu, Y.; Wang, S.; Liu, L. Experimental study on thermoelectric power generation based on cryogenic liquid cold energy. *Energy* **2021**, *220*, 119746. [CrossRef]
27. Liu, W.; Wang, D.-Z.; Liu, Q.; Zhou, W.; Shao, Z.; Chen, Z.-G. High-Performance GeTe-Based Thermoelectrics: From Materials to Devices. *Adv. Energy Mater.* **2020**, *10*, 2000367. [CrossRef]
28. Li, M.; Sun, Q.; Xu, S.D.; Hong, M.; Lyu, W.Y.; Liu, J.X.; Wang, Y.; Dargusch, M.; Zou, J.; Chen, Z.G. Optimizing Electronic Quality Factor toward High-Performance $Ge_{1-x-y}Ta_xSb_yTe$ Thermoelectrics: The Role of Transition Metal Doping. *Adv. Mater.* **2021**, *33*, e2102575. [CrossRef]
29. Chen, W.-Y.; Shi, X.-L.; Zou, J.; Chen, Z.-G. Wearable fiber-based thermoelectrics from materials to applications. *Nano Energy* **2021**, *81*, 105684. [CrossRef]
30. Nazari, S.; Safarzadeh, H.; Bahiraei, M. Performance improvement of a single slope solar still by employing thermoelectric cooling channel and copper oxide nanofluid: An experimental study. *J. Clean. Prod.* **2019**, *208*, 1041–1052. [CrossRef]